

Dalton Transactions

Accepted Manuscript



This is an *Accepted Manuscript*, which has been through the Royal Society of Chemistry peer review process and has been accepted for publication.

Accepted Manuscripts are published online shortly after acceptance, before technical editing, formatting and proof reading. Using this free service, authors can make their results available to the community, in citable form, before we publish the edited article. We will replace this *Accepted Manuscript* with the edited and formatted *Advance Article* as soon as it is available.

You can find more information about *Accepted Manuscripts* in the [Information for Authors](#).

Please note that technical editing may introduce minor changes to the text and/or graphics, which may alter content. The journal's standard [Terms & Conditions](#) and the [Ethical guidelines](#) still apply. In no event shall the Royal Society of Chemistry be held responsible for any errors or omissions in this *Accepted Manuscript* or any consequences arising from the use of any information it contains.



Journal Name

ARTICLE

Aggregation-Induced Emission (AIE) active probe for multiple targets: Fluorescent sensor for Zn²⁺ and Al³⁺ & colorimetric sensor for Cu²⁺ and F⁻

Received 00th January 20xx,
Accepted 00th January 20xx

DOI: 10.1039/x0xx00000x

www.rsc.org/

Soham Samanta,^a Utsab Manna,^a Turjya Ray^a and Gopal Das^a

A rationally designed probe **L**, consist of both cation and anion binding sites, is capable of displaying interesting aggregation induced emission (AIE) property. **L** not only can sense Al³⁺ and Zn²⁺ through selective turn-on fluorescence responses in 9:1 methanol-HEPES buffer (5mM, pH 7.3; 9:1, v/v) medium due to metal ion triggered AIE activity, but also can distinguish them through individual emission signals. **L** can also detect Cu²⁺ in mixed buffer medium and F⁻ in acetonitrile through sharp colorimetric responses. All the sensing processes are conspicuous through naked eye. Theoretical study strongly backed the proposed sensing mechanisms.

Introduction

Zinc, an essential element in human body, is involved in several biological processes, for instance cellular metabolism, gene transcription, regulation of metalloenzymes, neurotransmission, and apoptosis.¹ Despite its several crucial roles in many Zn(II)-containing enzymes and DNA-binding proteins, imbalance of Zn²⁺ in body may cause several neurological diseases.² Particularly in children under the age of 5 years, deficiency of Zn(II) could eventually lead to immune dysfunction, diarrhoea, and even death in some cases.³ Zinc, being a harmful pollutant for environment, also raises concern over its open exposure.⁴ Thus designing an efficient Zn²⁺ sensor is indispensable. Difficulties in developing Zn²⁺ sensors^{5a,5b} in many cases suffer from a limited choice of spectroscopic instruments due to its inherent d¹⁰ shell, poor selectivity or sensitivity, and interference from other d¹⁰ metal ions like Cd²⁺ and Hg²⁺.^{5c,5d} Hence, to develop highly selective and sensitive zinc sensors, workable in physiological condition would be of great interest.

Aluminium, the third most abundant metal in the earth's crust is widely known as a neurotoxic agent.⁶ Aluminium toxicity could adversely affect the central nervous system of human to induce Alzheimer's disease, Parkinson's disease, and amyotrophic lateral sclerosis.⁷ Meanwhile, the widespread use of Aluminium in medicines (antacids), bleached flour, paper industry, food additives, aluminum-based pharmaceuticals, storage/cooking utensils, makes it vulnerable to be exposed to

the environment in its trivalent ion form Al³⁺ which often causes drinking water contamination.⁸ Thus developing an efficient chemo-sensor for rapid and sensitive detection of Al³⁺ has earned great scientific interest amongst analytical chemists at large.

Fluorescence based sensing probes are advantageous over other sensing systems for the detection of biological and environmentally relevant metal ions as they can provide more rapid, convenient and sensitive detection of target analytes.⁹ Fluorescent probes, displaying aggregation-induced emission (AIE) have grabbed tremendous attention in very recent time. Though these probes display weak emission in dilute solutions, their emission intensity enhances dramatically due to the aggregation facilitated by probe–target interaction in solution or in the solid state. Hence, AIE active probes, that could yield enhancement in fluorescence instead of quenching on aggregation, have become very attractive candidates for robust and quantitative sensing of various biologically and environmentally important target analytes.¹⁰

On the other hand, copper, an essential trace element of human body and being present in the active sites of several enzymes, plays many indispensable role to sustain important physiological processes.¹¹ Copper deficiency increases the risk of coronary heart disease whereas overdose of copper could lead to detrimental effects by causing oxidative stress and disorders associated with neurodegenerative diseases including Alzheimer, Parkinson, Menkes, Wilson, and prion diseases.^{12,13} Thus rapid visual sensing Cu²⁺ in physiological condition is much anticipated.

Fluoride is recognized as one of the biologically as well as environmentally important anions. Though at low concentration fluoride could help in treating osteoporosis and protecting dental health, it apparently becomes toxic at higher doses. Several types of diseases in humans, caused due to the intake of high concentration of the fluoride anion in drinking

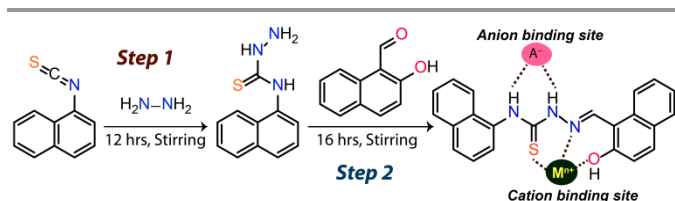
^a Department of Chemistry, Indian Institute of Technology Guwahati, Guwahati 781039, India. Fax: + 91 361 2582349; Tel: +91 3612582313; E-mail: gdas@iitg.ernet.in.

† Electronic Supplementary Information (ESI) available: [[NMR, HRMS characterization spectra of the probe, supporting plot and figures, DFT optimized structures.]]. See DOI: 10.1039/x0xx00000x

Dalton Transactions Accepted Manuscript

water are being tracked over the years. Fluoride toxicity also leads to fluorosis.¹⁴ In this context, design and synthesis of simpler organic probe for visible detection of F⁻ is much expected. A thorough literature survey revealed that there are very few reported fluoride ion selective optical probe.¹⁵ Vazquez *et. al.* developed an effective simple thiourea based optical probe where they demonstrated that the interaction of the thiourea hydrogen atoms with fluoride could enhance π - π^* delocalization and thereby shifted the π - π^* transition from the UV to the visible region to display yellow color.^{15b} Similarly, Ambrosi *et. al.* has also demonstrated the selective off-on fluorescence response of a coumarin-urea derived probe towards fluoride ion.^{15c} Visible detection of fluoride ion by a core-substituted naphthalene di-imide probe has also been reported recently.^{15d} However, probes with urea/thiourea moiety are found to be more useful for selective sensing of fluoride ion in solution. Thus designing a thiosemicarbazone probe consist of thiourea group could potentially be envisioned as a fluoride sensor.

Moreover, designing a versatile molecule that produces different fluorescence or colorimetric responses for different analytes can simultaneously be used to detect more than one analytes. Thus development of a multi-analyte sensor provides the scope for analytical time, labour and cost reduction.¹⁶ Recently, in this context, some thiosemicarbazone compounds have been used for selective sensing of various cations as well as anions.¹⁷



Scheme 1: Synthesis of Probe L.

In our constant pursuit to develop newer sensing probes¹⁸ for various biological and environmentally relevant analytes, here in we have designed a single versatile aggregation induced emission (AIE) active multiple target probe **L** that not only can fluorometrically sense Zn²⁺ and Al³⁺ in physiological conditions but also can distinguish one from another through individual fluorescence responses. The probe also demonstrated a selective colorimetric response towards Cu²⁺ in physiological condition. Alongside, the probe is also capable of displaying selective naked eye chromogenic detection of F⁻ in acetonitrile. The sensing behaviour of the probe was well supported with theoretical calculations.

Experimental section

General Information and Materials

All the materials for synthesis were purchased from commercial suppliers and used without further purification. The absorption spectra were recorded on a Perkin-Elmer Lambda-25 UV-vis spectrophotometer using 10 mm path length

quartz cuvettes in the range of 250–800 nm wavelength, while fluorescence measurements were performed on a Horiba Fluoromax-4 spectrofluorometer using 10 mm path length quartz cuvettes with a slit width of 3 nm at 298 K. The mass spectrum of the ligand **L** was obtained using Waters Q-ToF Premier mass spectrometer. Nuclear magnetic resonance (NMR) spectra were recorded on a Bruker Advance 600 MHz NMR instrument. The chemical shifts were recorded in parts per million (ppm) on the scale. The following abbreviations are used to describe spin multiplicities in ¹H NMR spectra: s = singlet; d = doublet; t = triplet; m = multiplet.

Synthesis of L

5 mmol of 1-Naphthyl isothiocyanate was dissolved in 30 ml THF solution and then to it excess of hydrazine hydrate (50 mmol) was added at once. Then the mixture solution was stirred for 12 hours to get a faint yellow-white precipitate (scheme 1, step 1). Then 1 mmol of the product obtained in step1 was dissolved in pure ethanol and to it 1 mmol of 2-hydroxy-1-naphthaldehyde was added. The mixture was then stirred for 16 hours to get a pale yellow precipitate which was collected by filtration and washed thoroughly by methanol and the product was dried in desiccator. The calculated yield of **L** was found to be 82%.

¹H NMR [600 MHz, DMSO-*d*₆, TMS, J (Hz), δ (ppm)]: 12.86 (1H, s), 11.15 (1H, s), 9.89 (1H, s), 9.07 (1H, s), 8.61 (1H, d, J=8.4), 8.03 (1H, d, J=9.0), 7.91 (1H, d, J=8.4), 7.72-7.70 (2H, m), 7.61 (1H, t, J=7.2), 7.44-7.40 (3H, m), 7.26 (1H, d, J=8.4), 7.01-6.97 (3H, m). ¹³C NMR [150 MHz, DMSO-*d*₆, TMS, δ (ppm)]: 162.74, 162.40, 161.79, 160.13, 158.61, 134.81, 133.17, 132.26, 131.06, 128.89, 128.02, 127.82, 123.81, 121.70, 119.58, 118.72, 118.17, 116.59, 108.36. ESI-MS (positive mode, m/z) Calculated for C₂₂H₁₁N₃OS: 372.1092 Found: 372.1067 [(M+H⁺)].

UV-Vis and fluorescence spectroscopic studies for metal ion (Zn²⁺, Al³⁺ and Cu²⁺) sensing

Stock solutions of various ions (1 × 10⁻¹ mol·L⁻¹) were prepared in deionized water. A stock solution of **L** (5 × 10⁻³ mol·L⁻¹) was prepared in DMSO. The solution of **L** was then diluted to 10 × 10⁻⁶ mol·L⁻¹ and 20 × 10⁻⁶ mol·L⁻¹ with CH₃OH/aqueous HEPES buffer (5mM, pH 7.3; 9:1, v/v) for the fluorescence experiments and UV-Visible experiments respectively. In UV-Visible selectivity experiment, the test samples were prepared by placing appropriate amounts of the stock solutions of the respective cations into a quartz optical cell of 1 cm path length filled with 1.0 mL of probe solution (20 × 10⁻⁶ mol·L⁻¹). In fluorescence selectivity experiment, the test samples were prepared by placing appropriate amounts of the stock solutions of the respective cations into 2.0 mL of probe solution (10 × 10⁻⁶ mol·L⁻¹). For UV-Visible and fluorescence titration experiments two different sets of metal ions (Zn²⁺, Al³⁺ and Cu²⁺) standard solutions having 1mM and 5mM concentrations were prepared by diluting the earlier prepared stock solutions (1 × 10⁻¹ mol·L⁻¹) in 9:1 methanol-water medium. Quartz optical cells of 1 cm path length were filled with 1.0 mL and 2.0 mL solutions of **L** for UV-Visible and

fluorescence titration experiments respectively, to which the (1mM and 5mM) ion stock solutions were gradually added using a micropipette. For fluorescence measurements, excitation was provided at 390 nm, and emission was acquired from 410 nm to 700 nm. Spectral data were recorded within 2 minutes after addition of the ions.

UV-Vis spectroscopic studies for anion (F^-) sensing

Stock solutions of various anions ($1 \times 10^{-1} \text{ mol}\cdot\text{L}^{-1}$) were prepared in methanol. A stock solution of **L** ($5 \times 10^{-3} \text{ mol}\cdot\text{L}^{-1}$) was prepared in DMSO. The solution of **L** was then diluted to $20 \times 10^{-6} \text{ mol}\cdot\text{L}^{-1}$ with CH_3CN for the UV-Visible experiments. In the selectivity experiment, the test samples were prepared by placing appropriate amounts of the stock solutions of different anions into a quartz optical cell of 1 cm path length filled with 1.0 mL of probe solution ($20 \times 10^{-6} \text{ mol}\cdot\text{L}^{-1}$). In the titration experiment, a quartz optical cell of 1 cm path length was filled with a 1.0 mL solution of **L** to which another sets of fluoride ion stock solutions (5mM, prepared in methanol by diluting the previous stock solution) was gradually added using a micropipette.

Calculation of detection limit

The detection limits were calculated on the basis of the fluorescence titrations. The fluorescence emission spectrum of **L** was measured 10 times, and the standard deviation of blank measurement was achieved. To gain the slope, the fluorescence emission at 523 nm was plotted as a concentration of Al^{3+} and the fluorescence emission at 494 nm was plotted as a concentration of Zn^{2+} . The detection limits were calculated using the following equation-

$$\text{Detection limit} = 3\sigma/k \quad (1)$$

Where σ is the standard deviation of blank measurement, and k is the slope between the fluorescence emission intensity versus $[\text{Zn}^{2+}]$ or, emission intensity versus $[\text{Al}^{3+}]$.

Job's plot experiment with UV-Vis method

Ten sets of 2 mL CH_3OH /aqueous HEPES buffer (5mM, pH 7.3; 9:1, v/v) solution were prepared with label 1 to 10. Now appropriate amount of ligand stock solutions were ($5 \times 10^{-3} \text{ mol}\cdot\text{L}^{-1}$) added to each set of solution so that the concentration of **L** in the solutions varies from $100\mu\text{M}$ to $10\mu\text{M}$ respectively in the ten vials. Then appropriate amount of Cu^{2+} solution ($5 \times 10^{-3} \text{ mol}\cdot\text{L}^{-1}$) added to each set of solution so that the concentration of Cu^{2+} in the solutions varies from $0\mu\text{M}$ to $90\mu\text{M}$ respectively in the ten vials. In each set the total concentration (metal + ligand) was kept constant at $100\mu\text{M}$. Now, UV-Vis spectra of all these 10 sets of solutions were recorded and from that absorbance at 456 nm were plotted against the mole fraction of Cu^{2+} to get Job's plot.

Dynamic light scattering studies

The particle size of **L**, **L-Al**³⁺ and **L-Zn**²⁺ aggregates were measured by dynamic light scattering (DLS) experiments on a Malvern Zetasizer Nano ZS instrument equipped with a 4.0 mW He-Ne laser operating at a wavelength of 633 nm. The

samples and the background were measured at room temperature (25°C) at a scattering angle of 173° . DLS experiments were carried out with optically clear solutions of **L** ($10 \mu\text{M}$) in 9:1 MeOH-H₂O and 1:9 MeOH-H₂O to observe the change in particle size upon increasing water fraction. DLS studies were also carried out with an optically clear solution of **L** ($10 \mu\text{M}$) in 9:1 MeOH-H₂O, in the presence of 20 equivalents of Al^{3+} and Zn^{2+} ion separately to determine the changes in particle size on interaction of **L** with these metal ions. The solution was equilibrated for 30 minutes before taking the measurements.

Results and Discussions

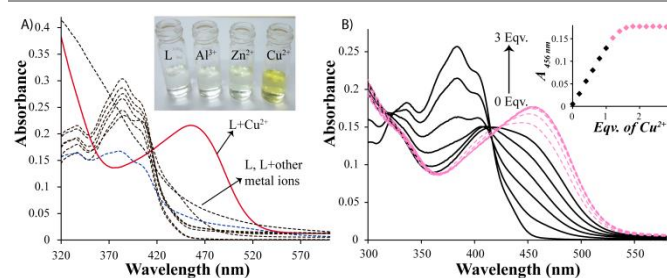


Figure 1: (A) UV-Visible spectra of **L** ($20\mu\text{M}$) in presence of 10 equivalents of various metal ions in CH_3OH /aqueous HEPES buffer (5mM, pH 7.3; 9:1, v/v) medium; Inset: Visual changes of the solution of **L** ($20\mu\text{M}$) in presence of Al^{3+} , Zn^{2+} and Cu^{2+} ions. (B) UV-Visible titration spectra of **L** ($20\mu\text{M}$) with incremental addition of Cu^{2+} ion in CH_3OH /aqueous HEPES buffer (5mM, pH 7.3; 9:1, v/v) medium, Inset: Change in absorbance at 456 nm with the equivalents of Cu^{2+} added into the solution.

The probe **L** was synthesized with good yield and in pure form by multi-step reactions (scheme 1). The design principle for the probe to sense multi-analytes is based on the following fundamental features: (1) The probe should contain chromophore/fluorophore with an excitation/emission in the relatively higher wavelength to get rid of the interference from biological systems and (2) it should possess both the cation and anion binding sites within a single molecule. Extensive UV-visible and fluorescence spectroscopic studies were perused to harvest the selective optical responses of **L** towards various cations and anions.

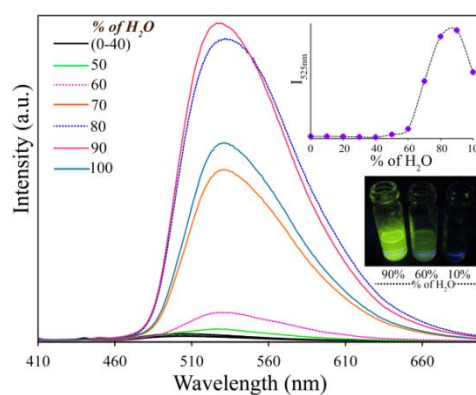


Figure 2: Emission spectra of **L** ($10\mu\text{M}$) upon changing the water fraction of methanol-water mixed solvent; $\lambda_{\text{ex}} = 390 \text{ nm}$. Inset: Change in the emission intensity at 525 nm and visual changes in fluorescence (under UV light) with different water fractions.

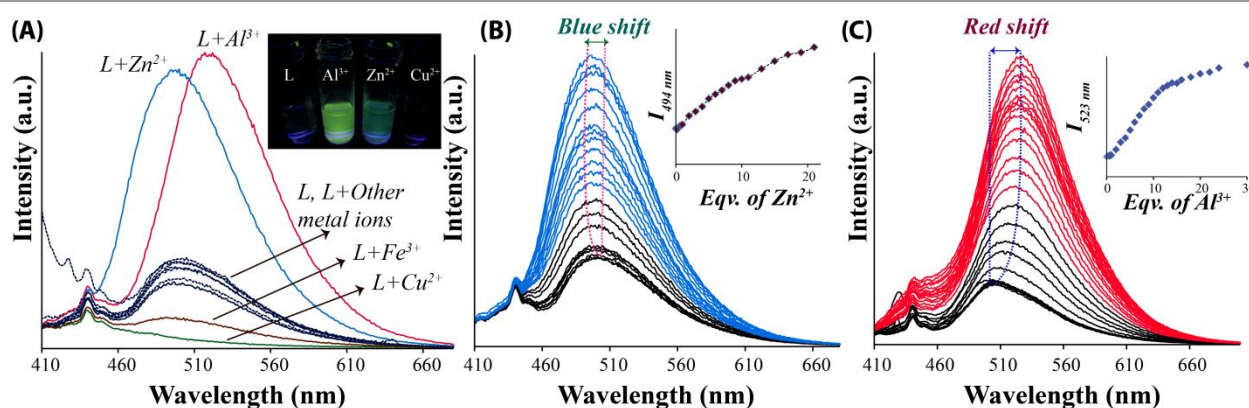


Figure 3: A) Fluorescence spectra of **L** (10 μ M) in CH_3OH /aqueous HEPES buffer (5 mM, pH 7.3; 9:1, v/v) medium in presence of 20 equivalents of different metal ions. INSET: Visual changes observed for **L** in presence of Al^{3+} , Zn^{2+} and Cu^{2+} ions under UV light. B) Fluorescence titration spectra of **L** (10 μ M) with incremental addition of Zn^{2+} in CH_3OH /aqueous HEPES buffer (5 mM, pH 7.3; 9:1, v/v) medium. INSET: Changes in the emission intensity at 494 nm with different concentration of Zn^{2+} ion. C) Fluorescence titration spectra of **L** (10 μ M) with incremental addition of Al^{3+} in CH_3OH /aqueous HEPES buffer (5 mM, pH 7.3; 9:1, v/v) medium. INSET: Changes in the emission intensity at 523 nm with different concentration of Al^{3+} ion. $\lambda_{\text{ex}} = 390$ nm.

Interaction of metal ions with **L**: UV–Vis spectroscopic studies

UV-Visible spectra of **L** revealed a broad absorbance maximum at 405 nm and a sharp absorbance maximum at 384 nm in CH_3OH /aqueous HEPES-buffer (5 mM, pH \sim 7.3; 9:1, v/v) medium, which might be attributed to the presence of naphthalene chromophore in the probe (Figure 1A). The selectivity of **L** was checked with chloride, nitrate or perchlorate salts of various metal ions which encompassed Na^+ , K^+ , Ca^{2+} , Mg^{2+} , Cr^{3+} , Hg^{2+} , Cu^{2+} , Pb^{2+} , Zn^{2+} , Fe^{3+} , Al^{3+} , Co^{2+} , Ni^{2+} , Cd^{2+} and Ag^+ . Addition of Cu^{2+} to **L** yielded characteristic colorimetric change as a new absorbance maximum emerged at 456 nm, with the concurrent disappearance of the original peaks at 405 nm and 384 nm (Figure 1A). Though, addition of Co^{2+} , Fe^{3+} and Zn^{2+} also brought slight spectral change to the UV-Visible spectra of **L**, those changes were very insignificant compared to colorimetric change induced by Cu^{2+} . All other metal ions hardly influenced the spectral property of **L**. Thus ligand **L** can sense Cu^{2+} through selective colorimetric response. Interestingly the spectral response of **L** toward Cu^{2+} was accompanied by a sharp visual color change of the experimental solution from almost colorless to yellow, which provided the scope for naked eye visible detection of Cu^{2+} (Figure 1A, Inset). To get a quantitative appraisal of the interaction between **L** and Cu^{2+} a titration experiment was carried out (Figure 1B). The gradual incremental addition of Cu^{2+} to **L** rendered a systematic growth of the absorbance maxima at 456 nm with a simultaneous downfall of the peaks at 384 nm and 405 nm. It is to be noted that a well-defined isosbestic point was generated at around 420 nm up to addition of 1 equivalent of Cu^{2+} (spectra with solid black traces

in Figure 1B). With the addition of excess amount of Cu^{2+} results in a slight deviation from the isosbestic point (spectra with dotted pink lines in Figure 1B). Thus initially the selective colorimetric response of **L** towards Cu^{2+} might be attributed to the chelation between **L** and Cu^{2+} ion. Job's plot obtained from the titration experiment (Figure S5, ESI) hinted towards an approximate 1:1.2 complex formation between **L** and Cu^{2+} . However, a conventional Job's plot experiment (detailed as mentioned in experimental section) has directly validated a 1:1 complex formation between **L** and Cu^{2+} (Figure S6, ESI). Thus the appearance of the absorption band at 456 nm with Cu^{2+} plausibly attributed to the deprotonated naphthol to metal charge transfer (LMCT) where the metal chelation facilitated the deprotonation of the naphthol moiety. The binding constant for the formation of **L**– Cu complex is calculated using the B–H (Benesi–Hildebrand) method, on the basis of change in absorbance at 456 nm, considering a 1:1 binding stoichiometry between **L** and Cu^{2+} . The binding constant was found to be $3.33 \times 10^4 \text{ M}^{-1}$ (Figure S7, ESI). This high binding constant value also endorsed the strong binding affinity of **L** toward Cu^{2+} in solution. Hence the probe **L** is capable of detecting Cu^{2+} through a selective colorimetric response, even conspicuous by naked eye. The detection limit was calculated according to the IUPAC method¹⁹ and it was found to be $4.64 \times 10^{-6} \text{ M}$ or, 0.29 ppm (Figure S8, ESI) which is way below the US-EPA permissible limit of Cu^{2+} in drinking water.

Interaction of metal ions with L: Fluorescence spectroscopic studies

L is very weakly emissive in pure methanol. Interestingly weakly emissive L in methanol became highly emissive in a methanol–water mixture with higher water content (Figure 2). Dynamic light scattering (DLS) studies of L in a mixed aqueous media suggested that the average particle size increased to 1545 nm from 612 nm with increasing water content of the medium from 10% to 90%. These results strongly recommended that L is an aggregation induced emission (AIE) active compound. As the water fraction above 50% only could lead to aggregation of L in medium itself (Figure 2, inset), all the fluorescence experiments in presence of metal ions were performed in 9:1 methanol–aqueous HEPES buffer medium, where the ligand itself does not show AIE activity on its own.

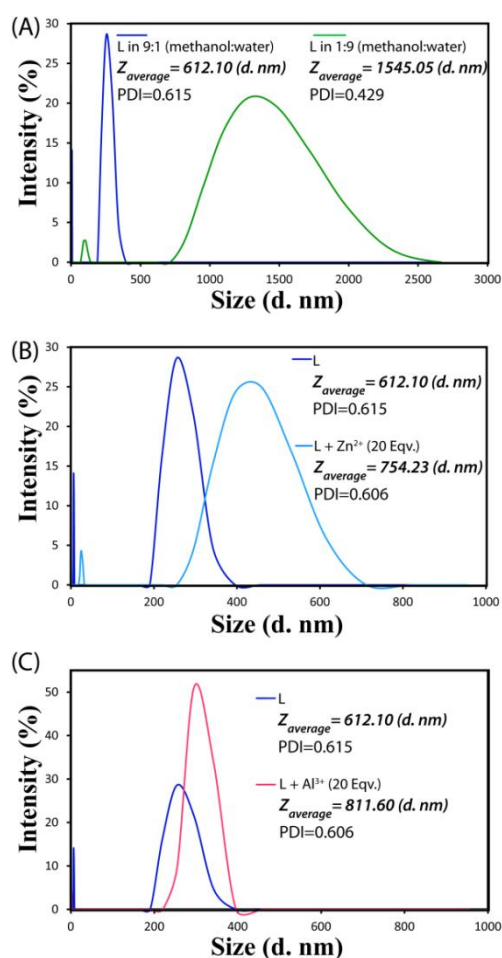
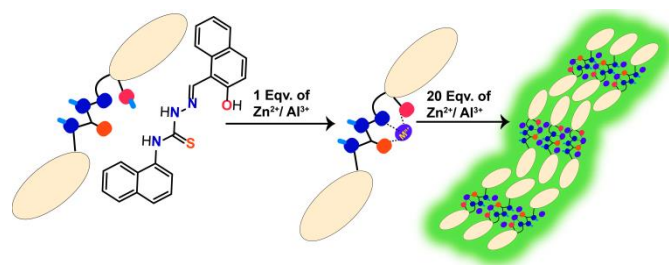


Figure 4: DLS-based particle size analysis of L (10 μM) (A) upon changing the solvent from 9:1 methanol–water to 1:9 methanol–water, (B) upon addition of 20 equivalents of Zn²⁺ ion. (C) upon addition of 20 equivalents of Al³⁺ ion.

A weak emission band at 501 nm was observed when L was excited at 390 nm in mixed solvents. The binding selectivity of L was perused with chloride, nitrate or perchlorate salts of various metal ions, as mentioned earlier. It was interesting to note that amongst all tested metal ions only Al³⁺ and Zn²⁺ rendered significant TURN-ON fluorescence responses (Figure 3A). Addition of Al³⁺ to L manifested a 22 nm red shifted new

peak at 523 nm along with a ~4 fold increase in fluorescence intensity. On the other hand, interaction of Zn²⁺ with L witnessed emergence of a 7 nm blue shifted emission maximum at 494 nm also accompanied by ~3.8 fold enhancement in fluorescence intensity (Figure 3A). Moreover, naked eye detection of these selective individual TURN-ON responses of L toward Al³⁺ and Zn²⁺ was also feasible under UV light, which rendered a bright yellowish green fluorescence for Al³⁺ and a bluish-green fluorescence for Zn²⁺ (Figure 3A, inset).



Scheme 2: Plausible sensing mechanism for metal ions.

However, the TURN-ON fluorescence response of L either in the presence of Al³⁺ or Zn²⁺ ion was interfered moderately by Cu²⁺, Co²⁺ and Fe³⁺ ions. Thus there is a scope for interference free sensing of Al³⁺ and Zn²⁺ in presence of all other metal ions except Cu²⁺, Co²⁺ and Fe³⁺ in 9:1 methanol–aqueous HEPES buffer medium (Figure S9, ESI). To get a quantitative appraisal of the relation between the change in fluorescence of L and the amount of metal ions interacted with it, detailed fluorescence titration experiments were conducted with both Al³⁺ as well as Zn²⁺. It was observed that the incremental addition of Al³⁺ or Zn²⁺ to L resulted in a systematic gradual enhancement of the fluorescence intensity (Figure 3B & 3C). However, contrary to the generation of the 22 nm red shifted emission maxima in case of titration experiment with Al³⁺, fluorescence titration with Zn²⁺ witnessed formation of the 7 nm blue shifted emission maxima.

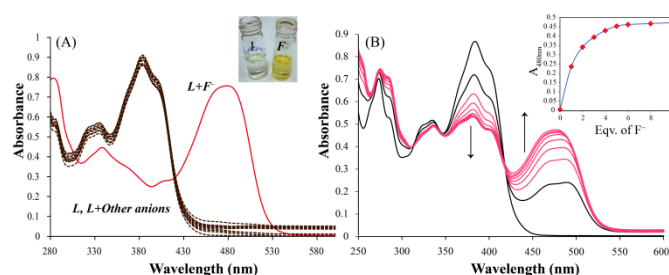


Figure 5: UV-visible spectra of L (20 μM) in presence of 10 equivalents of different anions in acetonitrile. Inset: Visual changes observed for L in presence of fluoride ion under daylight. (B) UV-vis spectra of L (20 μM) in presence of varying concentration of fluoride ion in acetonitrile. INSET: Changes in the absorbance at 480 nm with incremental addition of F⁻ ion.

Mass spectrum analysis confirmed the formation of a 1:1 L–Al³⁺ complex (Figure S10, ESI) as well as a 1:1 L–Zn²⁺ complex (Figure S11, ESI) with the generation of molecular ion peaks at $m/z = 478.33$ ([Al + L + H₂O + NO₃]⁺) and $m/z = 490.85$ ([Zn + L + 3H₂O]⁺) respectively.

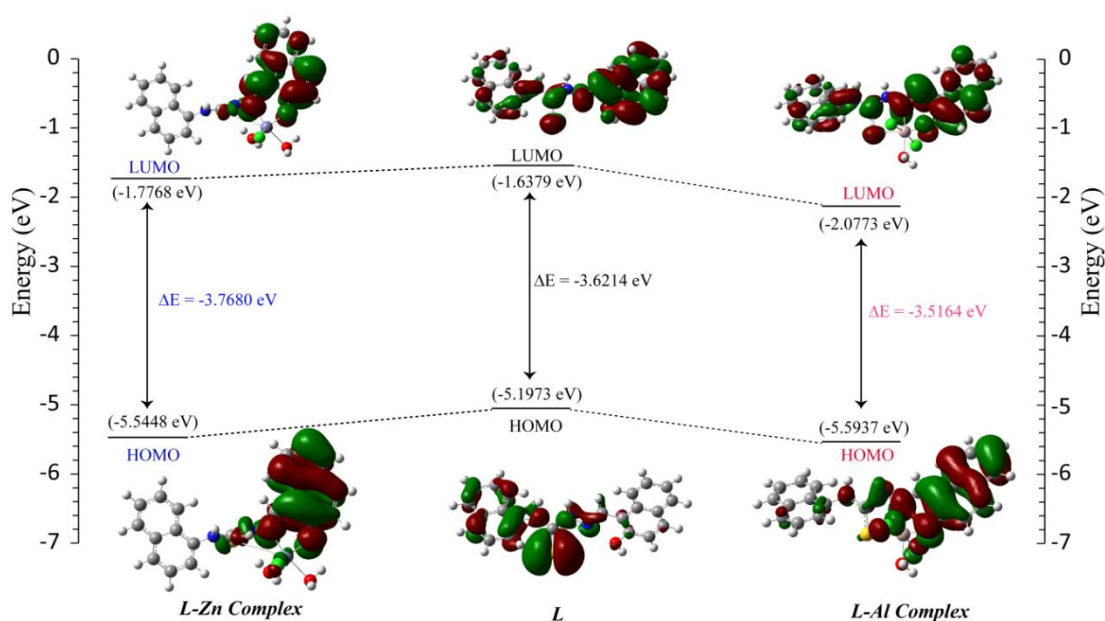


Figure 5: Frontier molecular orbital plots and energy level diagrams of L, L-Zn²⁺ complex and L-Al³⁺ complex. The calculations were performed using B3LYP/6-31 G (d,p) as implemented on Gaussian 03.

¹H NMR experiments of the ligand **L** were also carried out in presence of Al³⁺ and Zn²⁺. NMR experiments too supported the chelation phenomena, as the –OH peak of **L** at ~ 12.9 ppm broadened substantially after addition of the metal ions (Al³⁺ and Zn²⁺), which actually imply that –OH was deprotonated during complexation with either of the metal ions (Figure S12, S13; ESI). The detection limits for Al³⁺ and Zn²⁺ were calculated according to the IUPAC convention using equation 1, and those were found to be 6.86×10⁻⁷ M (Figure S14, ESI) and 1.03×10⁻⁶ M for Al³⁺ and Zn²⁺ (Figure S15, ESI) respectively, which are well below the USEPA permissible level of Al³⁺ and Zn²⁺ in drinking water.

Presumably, metal chelation was held responsible for the selective turn on fluorescence responses for Al³⁺ and Zn²⁺ as mass spectra indicated formation of a 1:1 L–Al³⁺ and L–Zn²⁺ complex. However, fluorescence titration experiment for both Al³⁺ and Zn²⁺ downplayed the possibility of simple coordination between **L** with Al³⁺ or Zn²⁺ by showing steady enhancement of the emission intensity of **L** up to addition of 20–30 equivalents of concerned metal ions (Figure 3B & 3C). Thus there is a possibility that presence of excess Zn²⁺ or Al³⁺ facilitated the aggregation process in solution along with formation of complex in the initial stages, which subsequently triggered the AIE activity of **L** (Scheme 2).

Initially the complexation between **L** and Al³⁺/Zn²⁺ led to the red/blue shift respectively up to addition of 1 equivalent of the concerned metal ion; however further addition of metal ions both in case of Zn²⁺ and Al³⁺ actually assisted the aggregation of the already formed complexes to enable the AIE behavior of **L** and consequently revealed dramatic enhancement in the corresponding fluorescence intensities. Extensive dynamic light scattering (DLS) studies of **L** in a mixed aqueous media were performed to understand the aggregation behavior of **L**

in presence of excess of Al³⁺ and Zn²⁺. DLS studies revealed that the average particle size of the probe **L** in mixed-aqueous (9:1 methanol-water; v/v) is 612 nm (Figure 4). Excitingly average particle size increased from 612 nm to 811 nm in similar condition in presence of 20 equivalents of Al³⁺. The addition of 20 equivalents Zn²⁺ also resulted in substantial increase in the average particle size from 612 nm to 754 nm (Figure 4). These results also support the observed metal ion (Al³⁺ and Zn²⁺)-triggered AIE activity of the probe **L** (Figure 3A). It may be mentioned here that though a similar type of probe (only differ in use of phenol moiety in place of naphthol moiety),^{17b} reported by Tong and co-workers showed ratio-metric fluorescent response toward Zn²⁺ in aqueous ethanol; our sensing system is much more effective and versatile compared to that as it not only can sense Al³⁺ and Zn²⁺ through selective differential TURN-ON fluorescence responses but also can sense Cu²⁺ and fluoride via sharp colorimetric responses. Alongside, simply changing the phenol moiety by naphthol moiety induces the interesting aggregation induced emission (AIE) activity of the probe to influence the sensing mechanism.

Interaction of anions with L: UV–Vis spectroscopic studies

The ligand **L** has potential anion binding sites too. Thus it was prudent to peruse the spectral outcome of **L** in presence of various anions (Figure 5A). Hence, binding selectivity of **L** was checked in presence of various anions such as, F⁻, Br⁻, Cl⁻, I⁻, SO₄²⁻, HSO₄⁻, PF₆⁻, NO₃⁻, HPO₄⁻, H₂PO₄⁻, OAc⁻, ClO₄⁻ etc. It was astonishing to note that only the presence of excess (10 equivalents) tetra-butyl-ammonium salts of fluoride was able to induce significant colorimetric response in acetonitrile (Figure 5A) whereas all other anions hardly influenced the spectral nature of **L**. Interaction of fluoride with **L**, resulted in the emergence of a new absorbance maximum at 480 nm,

with subsequent disappearance of the original peak at 378 nm. Moreover, this spectral change was also accompanied by some visual change in color from colorless to orange (Figure 5A, Inset) which offers the scope for the naked eye detection of fluoride in organic medium.

Titration experiment was performed to get a quantitative insight of the interaction between **L** and F^- . The titration experiment revealed the systematic increase in the absorbance at 480 nm with concurrent fall of the absorbance at 378 nm with the gradual incremental addition of fluoride to **L** (Figure 5B). It may be mentioned here that addition of strong base (tetra-butyl ammonium hydroxide) to **L** also generated a new absorbance peak at around 462 nm which is in contrast to the absorbance peak generated at around 480 nm by fluoride in similar condition (Figure S16, ESI). Also the nature of spectral response of the two curves is quite different from each other. Meanwhile, mass spectral analysis advocated for the 1:1 complex formation between **L** and fluoride ion by showing molecular ion peak at $m/z = 494.88$ ($[L + F^- + 2CH_3CN + Na^+]$) (Figure S17, ESI). Thus presumably this selective colorimetric response towards fluoride ion is mainly attributed to the specific coordination of the basic fluoride anion with **L** through strong hydrogen bonding. NMR titration experiment revealed that addition of fluoride ion up to one equivalent, actually favored coordination process through strong hydrogen bonding, as the $-NH$ proton peaks became weakened and broadened (Figure S18, ESI) during this titration. Further addition of fluoride up to 2.0 equivalents, led to the deprotonation, and thus furnished a peak at ~ 15.5 ppm, corresponds to HF_2^- (Figure S18, ESI). Hence, the fluoride sensing may be attributed to the combined effect of coordination and deprotonation of the probe.

Density Functional Theory (DFT) calculations

Extensive Density functional theory (DFT) calculations were perused to get the theoretical aspects of the observed selective emission responses of **L** towards Al^{3+} and Zn^{2+} . DFT optimizations of **L** and its Zn^{2+} and Al^{3+} complexes were carried out with the B3LYP/6-31+G(d,p) method basis set using the Gaussian 03 program. The optimized structures, HOMO and LUMO of **L**, $L-Zn^{2+}$ complex and $L-Al^{3+}$ complex are presented in Figure 5. It was astonishing to note that there is an increase in the HOMO to LUMO energy gap in case of $L-Zn^{2+}$ complex whereas HOMO to LUMO energy gap decreases in case of $L-Al^{3+}$ complex compared to **L**. Hence, these changes in the energy gaps clearly backed strongly the observed blue shift in emission maxima in case of Zn^{2+} and red shift in emission maxima in case of Al^{3+} .

Thus theoretically it is also likely that chelation followed by subsequent aggregation leads towards the selective turn-on fluorescence responses for both Al^{3+} and Zn^{2+} .

Density functional theory (DFT) calculations were also carried out for $L-F^-$ and $L-Cu^{2+}$ complexes. For the $L-F^-$, the lowering in the energy of HOMO to LUMO energy gap also validated the generation of observed red shifted absorbance maximum at 480 nm (Figure S22, ESI). Similarly, in case of $L-Cu^{2+}$ complex crunch in the HOMO to LUMO energy gap supported the

emergence of the new red shifted absorbance maximum when Cu^{2+} was added to **L** (Figure S23, ESI). The optimized structures of all the complexes are provided in the ESI (Figure S24, ESI).

Conclusions

In summary, here in we have synthesized a new fluorogenic probe, which is capable of displaying interesting aggregation induced emission (AIE) active property. The probe can detect multiple targets at a time through differential colorimetric and fluorometric responses. It can selectively sense Cu^{2+} through sharp colorimetric output through 1:1 chelation. Alongside, **L** can sense Zn^{2+} and Al^{3+} in mixed buffer medium through individual selective turn-on fluorescence responses which might be attributed to the chelation mediated triggering of the AIE behaviour of the probe. Nevertheless, as probe contains anion binding sites also, it is capable of detecting fluoride through a selective chromogenic response in acetonitrile.

Acknowledgements

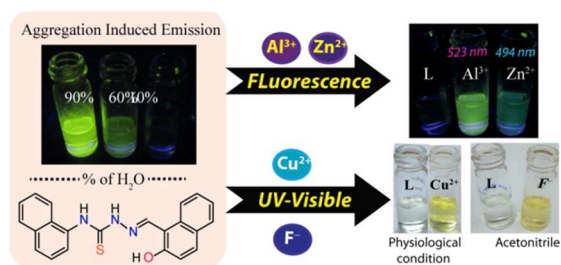
G.D. acknowledges CSIR (01/2727/13/EMR-II) and Science & Engineering Research Board (SR/S1/OC-62/2011), India for financial support, CIF IITG for providing instrument facilities. SS and UM acknowledge IIT Guwahati for fellowship.

Notes and references

- (a) E. L. Que, D. W. Domaille and C. J. Chang, *Chem. Rev.*, 2008, **108**, 1517; (b) C. J. Frederickson, J. Y. Koh and A. I. Bush, *Nat. Rev. Neurosci.*, 2005, **6**, 449; (c) A. G. Scrimgeour, C. H. Stahl, J. P. McClung, L. J. Marchitelli and A. J. Young, *J. Nutr. Biol.*, 2007, **18**, 813; (d) J. M. Berg and Y. Shi, *Science*, 1996, **271**, 1081.
- (a) Z. Xu, J. Yoon and D. R. Spring, *Chem. Soc. Rev.*, 2010, **39**, 1996; (b) P. Jiang and Z. Guo, *Coord. Chem. Rev.*, 2004, **248**, 205; (c) E. J. Song, H. Kim, I. H. Hwang, K. B. Kim, A. R. Kim, I. Noh and C. Kim, *Sens. Actuators B*, 2014, **195**, 36.
- M. Hambidge, *J. Nutr.*, 2000, **130**, 1344.
- A Voegelin, S Poster., A. C. Scheinost, M. A Marcus and R. Kretzschmar, *Environ. Sci. Technol.*, 2005, **39**, 6616.
- (a) D. Y. Zhang, M. Azrad, W. Demark-Wahnefried, C. J. Frederickson, S. J. Lippard, and R. J. Radford, *ACS Chem. Biol.*, 2015, **10**, 385; (b) A. Loas, R. J. Radford, and S. J. Lippard, *Inorg. Chem.*, 2014, **53**, 6491; (c) L. Xue, C. Liu and H. Jiang, *Org. Lett.*, 2009, **11**, 1655. (d) L. Xue, C. Liu and H. Jiang, *Org. Lett.*, 2009, **11**, 3454.
- (a) R. A. Yokel, *Fundam. Appl. Toxicol.*, 1987, **9**, 795; (b) G. Muller, V. Bernuzzi and D. Desor, *Teratology*, 1990, **42**, 253; (c) J. M. Donald and M. S. Golub, *Neurotoxicol. Teratol.*, 1989, **11**, 341.
- (a) A. Salifoglou, *Coord. Chem. Rev.*, 2002, **228**, 297. (b) M. E. Percy, T. P. A. Kruck, A. I. Pogue and W. J. Lukiw, *J. Inorg. Biochem.*, 2011, **105**, 1505; (c) G. D. Fasman, *Coord. Chem. Rev.*, 1996, **149**, 125. (d) D. Krewski, R. A. Yokel, E. Nieboer, D. Borchelt, J. Cohen, J. Harry S. Kacew, J. Lindsay, A. M. Mahfouz and V. Rondeau, *J. Toxicol. Environ. Health, Part B*, 2007, **10(S1)**, 1.
- (a) P. Jiang, L. Chen, J. Lin, Q. Liu, J. Ding, X. Gao and Z. Guo, *Chem. Commun.*, 2002, 1424; (b) S. Goswami, S. Paul and A. Manna, *RSC Adv.*, 2013, **3**, 10639; (c) A. Sahana, A. Benerjee,

- S. Lohar, A. Banik, S. K. Mukhopadhyay, D. A. Safin, M. G. Babashkina, M. Bolte, Y. Garcia and D. Das, *Dalton Trans.*, 2013, 13311; (d) D. Karak, S. Lohar, A. Sahana, S. Guha, A. Banerjee and D. Das, *Anal. Methods*, 2012, **4**, 1906; (e) G. D. Fasman, *Chem. Rev.*, 1996, **149**, 125; (f) P. Nayak, *Environ. Res.*, 2002, **89**, 101.
- 9 (a) J. Wang, W. Lin and W. Li, *Chem. Eur. J.* 2012, **18**, 13629; (b) J. Y. Zhang, B. L. Xing, J. Z. Song, F. Zhang, C. Y. Nie, L. Jiao, L. B. Liu, F. T. Lv and S. Wang, *Anal. Chem.* 2014, **86**, 346; (c) L. H. Feng, C. L. Zhu, H. X. Yuan, L. B. Liu, F. T. Lv and S. Wang, *Chem. Soc. Rev.* 2013, **42**, 6620; (d) L. Yuan, W. Lin, K. Zheng and S. Zhu, *Acc. Chem. Res.*, 2013, **46**, 1462.
- 10 (a) J. Luo, Z. Xie, J. W. Y. Lam, L. Cheng, H. Chen, C. Qiu, H. S. Kwok, X. Zhan, Y. Liu, D. Zhu and B. Z. Tang, *Chem. Commun.*, 2001, 1740; (b) Y. Hong, J. W. Y. Lam and B. Z. Tang, *Chem. Commun.*, 2009, 4332; (c) Y. Hong, J. W. Y. Lam and B. Z. Tang, *Chem. Soc. Rev.*, 2011, **40**, 5361.
- 11 (a) M. C. Linder and M. Hazegh-Azam, *Am. J. Clin. Nutr.*, 1996, **63**, 797S; (b) R. Uauy, M. Olivares and M. Gonzalez, *Am. J. Clin. Nutr.*, 1998, **67**, 952S; (c) G. E. Cartwright and M. M. Wintrobe, *Am. J. Clin. Nutr.*, 1964, **14**, 224; (d) D. G. Barceloux, *J. Toxicol., Clin. Toxicol.*, 1999, **37**, 217; (e) D. Strausak, J. F. Mercer, H. H. Dieter, W. Stremmel, and G. Multhaup, *Brain Res. Bull.*, 2001, **55**, 175.
- 12 (a) C. Vulpe, B. Levinson, S. Whitney, S. Packman and J. Gitschier, *Nat. Genet.*, 1993, **3**, 7; (b) D. J. Waggoner, T. B. Bartnikas and J. D. Gitlin, *Neurobiol., Dis.* 1999, **6**, 221; (c) J. S. Valentine and P. J. Hart, *Proc. Natl. Acad. Sci. U.S.A.*, 2003, **100**, 3617; (d) D. R. Brown and H. Kozlowski, *Dalton Trans.*, 2004, 1907; (e) K. J. Barnham, C. L. Masters and A. I. Bush, *Nat. Rev. Drug Discov.*, 2004, **3**, 205; (f) B. E. Kim, T. Nevitt and D. J. Thiele, *Nat. Chem. Biol.*, 2008, **4**, 176.
- 13 (a) G. J. Brewer, *Curr. Opin. Chem. Biol.*, 2003, **7**, 207; (b) G. L. Millhauser, *Acc. Chem. Res.*, 2004, **37**, 79; (c) S. P. Leach, M. D. Salman and D. Hamar, *Anim. Health Res. Rev.*, 2006, **7**, 97; (d) K. J. Barnham and A. I. Bush, *Curr. Opin. Chem. Biol.*, 2008, **12**, 222; (e) R. R. Crichton, D. T. Dexter and R. J. Ward, *Coord. Chem. Rev.*, 2008, **252**, 1189.
- 14 (a) T. Jentsch, *Curr. Opin. Neurobiol.*, 1996, **6**, 303; (b) A. Wiseman, *Handbook of Experimental pharmacology XX/2, Part 2*; Springer-Verlag: Berlin, 1970, 48; (c) J. A. Weatherall, *Pharmacology of Fluorides*. In *Handbook of Experimental pharmacology XX/2, Part 2*; Springer-Verlag: Berlin, 1969, 141; (d) R. H. Dreisbuch, *Handbook of Poisoning*; Lange Medical Publishers: Los Altos, CA, 1980.
- 15 (a) P. A. Gale, N. Busschaert, C. J. E. Haynes, L. E. Karagiannidis and I. L. Kirby, *Chem. Soc. Rev.*, 2014, **43**, 205; (b) M. Vazquez, L. Fabbri, A. Taglietti, R. M. Pedrido, A. M. Gonzalez-Noya and M. R. Bermejo, *Angew. Chem. Int. Ed.* 2004, **43**, 1962; (c) G. Ambrosi, M. Formica, V. Fusi, L. Giorgi, E. Macedi, G. Piersanti, M. Retini, M. A. Varrese and G. Zappia, *Tetrahedron*, 2012, **68**, 3768; (d) D. Buckland, S. V. Bhosale and S. J. Langford, *Tetrahedron Lett.*, 2011, **52**, 1990.
- 16 (a) L. Wang, H. Li and D. Cao, *Sens. Actuators B.*, 2013, **181**, 749; (b) M. Wang, J. Wang, W. Xue and A. Wu, *Dyes Pigm.*, 2013, **97**, 475; (c) P. N. Basa and A. G. Sykes, *J. Org. Chem.*, 2012, **77**, 8428; (d) H. J. Jung, N. Singh, D. Y. Lee and D. O. Jang, *Tetrahedron Lett.*, 2010, **51**, 3962; (e) A. Liu, L. Yang, Z. Zhang, Z. Zhang and D. Xu, *Dyes Pigm.*, 2013, **99**, 472; (f) C. Kar, S. Samanta, S. Goswami, A. Ramesh and G. Das, *Dalton Trans.*, 2015, **44**, 4123; (g) S. Samanta, S. Goswami, A. Ramesh and G. Das, *J. Photochem. Photobiol. A*, 2015, **310**, 45.
- 17 (a) M. J. C. Marenco, C. Fowley, B. W. Hyland, G. R. C. Hamilton, D. G. Riano and J. F. Callan, *Tetrahedron Lett.*, 2012, **53**, 670; (b) Z. Li, Y. Xiang and A. Tong, *Anal. Chim. Acta*, 2008, **619**, 75; (c) H. Su, W. Huang, Z. Yang, H. Lin and H. Lin, *J. Incl. Phenom. Macrocycl. Chem.* 2012, **72**, 221; (d) W. Radchatawedchakoon, W. Sangsuwan, S. Kruanetr and U. Sakee, *Spectrochim. Acta. A*, 2014, **121**, 306.
- 18 (a) C. Kar, M. D. Adhikari, A. Ramesh and G. Das, *Inorg. Chem.*, 2013, **52**, 743; (b) S. Samanta, S. Goswami, Md. N. Hoque, A. Ramesh and G. Das, *Chem. Commun.*, 2014, **50**, 11833; (c) S. Samanta, S. Goswami, Md. N. Hoque, A. Ramesh and G. Das, *Sens. Actuators B.*, 2014, **194**, 120; (d) S. Samanta, C. Kar and G. Das, *Anal. Chem.* 2015, **87**, 9002.
- 19 J. Lnczédy, T. Lengyel, and A. M. Ure, (Eds.), *IUPAC Compendium of Analytical Nomenclature, Definitive Rules*, 1997, web edition, IUPAC, 2002.

Graphical Abstract



A rationally designed aggregation-Induced Emission (AIE) active probe acts as a turn-on fluorescent sensor for Zn²⁺ and Al³⁺ besides a colorimetric sensor for Cu²⁺ and F⁻ ions